



Cite this: *J. Mater. Chem. A*, 2023, 11, 16363

## A dual functional molecule for perovskite/P3HT interface to achieve stable perovskite solar cells†

Hyuntae Choi,<sup>a</sup> Haeryang Lim,<sup>a</sup> Heesu Kim,<sup>b</sup> Jeongin Lim,<sup>b</sup> Minji Park,<sup>b</sup> Chandra Shakher Pathak<sup>id</sup><sup>b</sup> and Seulki Song<sup>id</sup><sup>\*b</sup>

After the introduction of spiro-OMeTAD as a hole transport material (HTM), the efficiency of perovskite solar cells (PSCs) has skyrocketed. However, dopants in spiro-OMeTAD make PSCs vulnerable to moisture and heat. Furthermore, the cost of spiro-OMeTAD is quite high, impeding the commercialization of PSCs. Therefore, the demand for HTMs that are dopant-free and cost-effective is increasing. In this regard, P3HT satisfies these criteria, exhibiting low-cost, long term stability, and high hole mobility. Despite these advantages, the PSCs with P3HT showed a lower efficiency compared to those PSCs with spiro-OMeTAD. Herein, we newly synthesized and employed a dual functional molecule, octylammonium azide (OAN<sub>3</sub>). The ammonium ion could interact with perovskite and passivate the defects in perovskite and the azide moiety could provide crosslinking sites with P3HT, improving both efficiency and long-term stability. As a result, the perovskite solar cells (PSCs) with OAN<sub>3</sub> obtained a maximum efficiency of 20.0%. In contrast, bare PSCs achieved a maximum efficiency of 13.8%. In addition, PSCs with OAN<sub>3</sub> maintained 90% and 82% of their initial efficiency under RH = 50–60% condition. However, the bare PSCs retained 38% of their initial efficiency under the same conditions.

Received 31st March 2023  
Accepted 5th July 2023

DOI: 10.1039/d3ta01910a

rs.c.li/materials-a

<sup>a</sup>Department of Chemical Engineering, Pohang University of Science and Technology (POSTECH), 77 Cheongam-Ro, Nam-gu, Pohang, Gyeongbuk, Korea 37673

<sup>b</sup>Department of Chemical Engineering and Applied Chemistry, Chungnam National University (CNU), 99 Daehak-Ro, Yuseong-gu, Daejeon, Republic of Korea 34134.

E-mail: sksong@cnu.ac.kr

† Electronic supplementary information (ESI) available. See DOI: <https://doi.org/10.1039/d3ta01910a>



*Prof. Seulki Song is an assistant professor in the Department of Chemical Engineering and Applied Chemistry at Chungnam National University. He obtained his Ph. D degree from the Department of Chemical Engineering at POSTECH (advisor: Prof. Taiho Park) in 2017 and worked at the Max-Planck Institute für Kohlenforschung (Germany, 2017–2018) as a postdoctoral fellow (advisor Dr*

*Harun Tüysüz). He also worked at the Korea Research Institute of Chemical Technology (KRICT) as a senior researcher (2018–2021). His current research focuses on thin film engineering of semiconductor materials and improvement of energy device efficiency and stability.*

## Introduction

The halide perovskite, well known as the ABX<sub>3</sub> structure (A: monovalent cation, B: divalent cation, and X: halides), has presented remarkable applicability to diverse optoelectronic devices such as solar cells, light emitting diodes, sensors, and laser.<sup>1–3</sup> Among them, perovskite solar cells (PSCs) showed incredible progress in the past decade, achieving a certified efficiency of 25.7% and are expected to be commercialized.<sup>4</sup> Currently, the commercialization of PSCs is a significant issue that cannot be postponed any longer in terms of climate change and eco-friendly energy shortage. However, to be commercialized, several issues remain, such as scalability, toxicity of lead, and instability issue.<sup>5</sup> In particular, the instability of PSCs is the major obstacle interrupting the commercialization of PSCs despite their excellent photovoltaic performance.<sup>6–9</sup>

To date, 2,2',7,7'-tetrakis[*N,N*-di(4-methoxyphenyl)amino]-9,9'-spirobifluorene (spiro-OMeTAD) is widely adopted as a hole transporting material (HTM) in the state-of-the-art PSCs.<sup>10–13</sup> However, spiro-OMeTAD requires dopants (*i.e.*, Li-TFSI and tBP) to improve the intrinsic low hole mobility.<sup>14,15</sup> These dopants could adversely affect the long-term stability of PSCs by facilitating the degradation of the perovskite material. In particular, Li-TFSI possesses a hygroscopic nature, which promotes the adsorption of moisture and perovskite degradation.<sup>16</sup> Moreover, tBP forms a complex with PbI<sub>2</sub> and causes the decomposition of the perovskite layer.<sup>17</sup> Even worse, tBP gradually evaporates at ambient conditions and could cause severe instability under

heat, deteriorating film morphology and performance of PSCs.<sup>18</sup> Owing to the aforementioned issues, introducing spiro-OMeTAD as an HTM results in poor long-term stability against moisture and heat.<sup>19,20</sup> Recently, to address these issues, novel doping strategies have been proposed to effectively oxidize spiro-OMeTAD without using Li-TFSI, including radical doping and CO<sub>2</sub> doping.<sup>21–23</sup> Although the stability is quite improved by adopting these methods, the long-term stability is still low. These problems are pointed out as a huge obstacle to realizing the commercialization of PSCs.<sup>24</sup>

Various strategies have been proposed, such as developing non-hygroscopic dopants,<sup>25,26</sup> fabricating bi-layer structure,<sup>27,28</sup> and synthesizing dopant-free HTMs, to improve the poor stability resulting from the conventional HTM model.<sup>29–33</sup> Among them, developing dopant-free HTM is a fundamental solution in that it is capable of achieving high efficiency and stability and realizing the commercialization of PSCs. However, most dopant-free HTMs require expensive monomers and many synthesis steps, which leads to high costs. In terms of cost-effectiveness and robust long-term stability, poly(3-hexylthiophene) (P3HT) was paid attention as a promising HTM.<sup>34</sup> In addition, P3HT exhibited high mobility, which is one of the significant factors in determining the performance of HTM.<sup>32</sup> However, when adopting P3HT, the perovskite film has to be contacted with alkyl side chains of P3HT, which leads to a poor interface between perovskite and P3HT.

This phenomenon induces non-radiative recombination and deteriorates the performance of PSCs.<sup>34,35</sup> In order to solve this problem, several researchers have introduced molecules at the interface between perovskite and P3HT.<sup>36,37</sup> In addition, doping P3HT with different small molecules is also a preferred strategy to improve efficiency.<sup>38–40</sup> Recently, different additives that could affect the packing and orientation are also devised: J. Seo and J. H. Noh group introduced alkyl halide-based small molecules to the top of perovskite film and controlled the packing of P3HT.<sup>34,41</sup> In addition, Hu group employed the SME-TATPYr molecule and improved the hole mobility by directly changing the packing of P3HT.<sup>42</sup> Recently, J. Gao group has constructed molecular bridges (MDN) to passivate the defects and form a charge transport channel.<sup>35</sup> However, these research studies have a limitation in that they have used a secondary bonding between the additive and P3HT, which is not strong enough compared to a covalent bond.

To effectively enhance the stability of PSCs, the perovskite surface, HTM, and interface between perovskite and HTM should all be considered. Defects existing in the perovskite surface must be well controlled, the interface with the HTM must be well formed, and the electrical properties of the HTM itself must also be maintained high. However, the studies controlling perovskite defects, perovskite/HTM interface and properties of HTM have been implemented individually. Research that could control the aforementioned three parts at once could be regarded as a core technology for the commercialization of PSCs.

To achieve this, we designed and synthesized a new dual functional interface modulating material, octylammonium

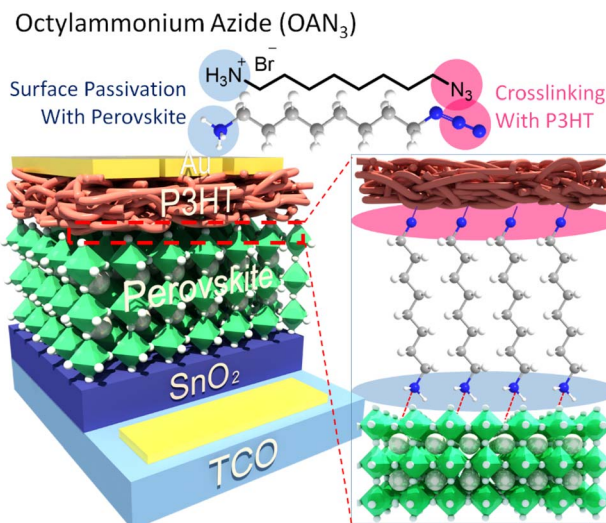


Fig. 1 Schematic illustration of perovskite solar cells with cross-linkable molecule, octylammonium azide (OAN<sub>3</sub>).

azide (OAN<sub>3</sub>) (Fig. 1). The ammonium ion has been reported to passivate the defects in perovskites.<sup>43,44</sup> In addition, the azide moiety could provide a crosslinking site with P3HT, strengthening the interfacial contact between perovskite and P3HT.<sup>45,46</sup> As a result, the P3HT with OAN<sub>3</sub> and bare PSCs showed a PCE of 20.0% and 13.8%, respectively, mainly resulting from increased open-circuit voltage ( $V_{OC}$ ) and fill factor (FF). Moreover, the PSCs treated with OAN<sub>3</sub> exhibited improved stability under humid conditions. The OAN<sub>3</sub> treated PSCs maintained 90% and 82% of their initial efficiency (with and without crosslinking, respectively) for 500 h under 50–60% relative humidity. In contrast, bare PSCs have retained only 38% of their initial efficiency. We believe that our dual functional molecule strategy could provide a guideline to achieve a stable and efficient perovskite solar cell.

## Results and discussion

The synthetic scheme and characterization of OAN<sub>3</sub> are provided in Scheme S1 and Fig. S1–S3.† Azide moiety is known to generate nitrene after UV light irradiation, inducing insertion reactions with C–H bonds.<sup>45,46</sup> The Fourier transform infrared (FT-IR) spectroscopy of OAN<sub>3</sub> with P3HT was performed to confirm the crosslinking after UV irradiation. The characteristic peak of azide groups *via* the asymmetric stretching band (N<sub>3</sub>) appeared in the 2000–2200 region (Fig. 2a).<sup>45,46</sup> After crosslinking, we could check that the corresponding peak is decreased. Furthermore, as the evidence of crosslinking, the C–H stretching peak increased (Fig. 2a). We could also confirm the crosslinking of the interface through UV-Vis spectra. We prepared the film with the configuration of glass/OAN<sub>3</sub>/P3HT (Fig. 2b). The absorbance of crosslinked P3HT is decreased after the first washing, as the crosslinking only occurred in the interface between OAN<sub>3</sub> and P3HT and not in the full P3HT film. When we measured the UV-Vis spectra after irradiation, the absorbance remained almost at its initial state even after three

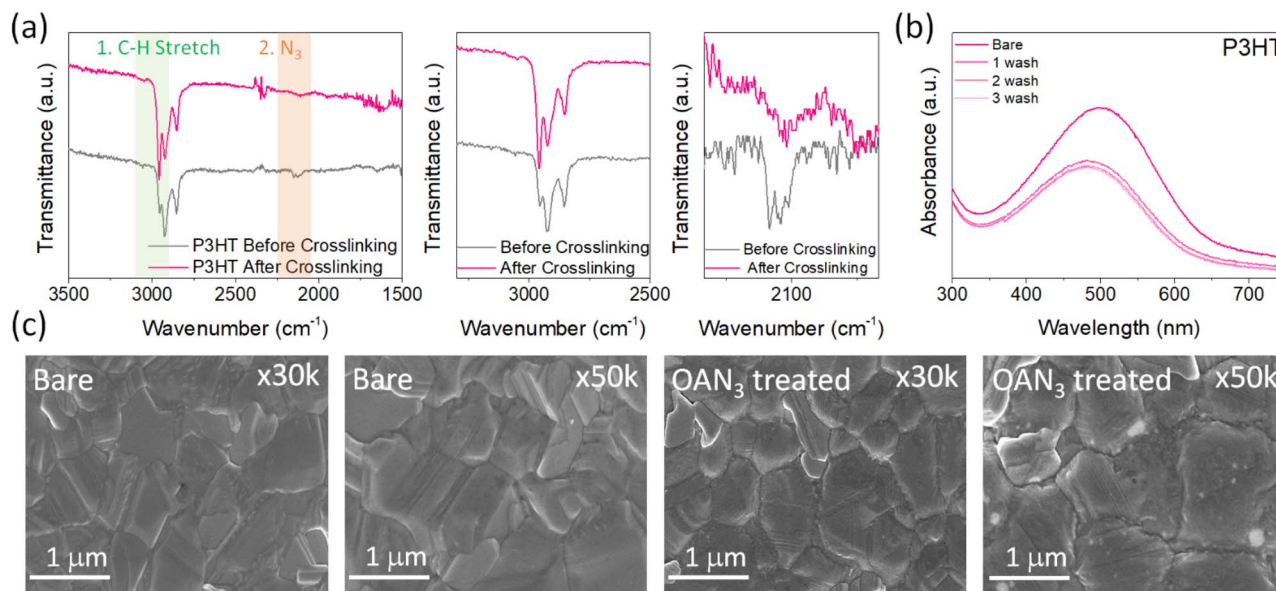


Fig. 2 (a) The FT-IR spectra before and after crosslinking. (b) UV-Vis spectra of P3HT after crosslinking and washing with chlorobenzene. (c) SEM images of perovskite film with different concentrations of OAN<sub>3</sub>.

times of washing, indicating the crosslinking proceeded. This phenomenon could also be confirmed by film images of washed P3HT before and after the crosslinking process (Fig. S4<sup>†</sup>). After confirming the crosslink ability of OAN<sub>3</sub>, we checked the interaction of OAN<sub>3</sub> with perovskite crystals. We used scanning electron microscope (SEM) to figure out the difference in the perovskite film surface after OAN<sub>3</sub> treatment (Fig. 2c). The grain size of perovskite film before and after OAN<sub>3</sub> are similar, indicating that the morphology of perovskite film is not significantly affected.

In addition, we measured X-ray photoelectron spectroscopy (XPS) to figure out the interaction between perovskite and OAN<sub>3</sub> (Fig. 3a). As a result, in the bare perovskite, the XPS peaks of Pb 4f appeared at 142.9 and 138.05 eV, respectively. In contrast, the XPS peaks of Pb 4f in the OAN<sub>3</sub> treated perovskite appeared at 142.65 and 137.8 eV. This result indicates that the ammonium ions in the OAN<sub>3</sub> molecule could interact with Pb atoms. Furthermore, Pb metallic peak (Pb<sup>0</sup>) is reduced (141.1 and 136.3 eV), which indicates the reduction of non-radiative recombination.<sup>47</sup> In addition, the peak shift of I 3d occurred, resulting from the hydrogen bond (N–H⋯I) interaction between N–H in OAN<sub>3</sub> and iodide in PbI<sub>2</sub> (Fig. S5<sup>†</sup>).<sup>48</sup> From the aforementioned XPS results, OAN<sub>3</sub> could interact with both Pb and I ions, respectively. We also measured the <sup>1</sup>H NMR for OAN<sub>3</sub> and the mixture of OAN<sub>3</sub> and PbI<sub>2</sub> (Fig. S6<sup>†</sup>). The peak from ammonium ion (7.77 ppm) in the bare OAN<sub>3</sub> shifted toward the up-field (7.69 ppm) after PbI<sub>2</sub> addition. This result could support the fact that the interaction between perovskite and OAN<sub>3</sub> exists. The positive effect of OAN<sub>3</sub> could be found in the X-ray diffraction (XRD) measurement (Fig. 3b). The perovskite film exhibits peaks at  $2\theta = 13.7^\circ$ ,  $28.0^\circ$ , and  $42.7^\circ$ , corresponding to the (100), (200), and (300) perovskite lattice planes.<sup>49</sup>

The crystallinity of perovskite crystal is increased after incorporating OAN<sub>3</sub>. In addition, the lifetime of charge carriers is elongated, as shown in the steady-state and time-resolved photoluminescence (SSPL and TRPL) (Fig. 3c and d). The TRPL measurement was performed with the configuration of glass/perovskite/OAN<sub>3</sub>. The  $\tau_1$  value of bare perovskite is 1.98 μs. In the meantime, the  $\tau_1$  value of perovskite treated with OAN<sub>3</sub> is 2.35 μs, indicating the reduction of the non-radiative recombination. In addition, we also measured the TRPL of the samples with the configuration of glass/perovskite/OAN<sub>3</sub>/P3HT to confirm the charge extraction ability of OAN<sub>3</sub> treatment (Fig. S7<sup>†</sup>). In the TRPL, the  $\tau_1$  value for OAN<sub>3</sub>-treated film was examined to be 0.43 ns, which is smaller than that of bare perovskite-base film (0.65 ns).<sup>50</sup> This result implies that the OAN<sub>3</sub> could facilitate charge transfer from perovskite to P3HT. Also, the absorbance of the perovskite treated with OAN<sub>3</sub> is slightly improved compared to bare perovskite (Fig. S8<sup>†</sup>). Lastly, to quantitatively measure the defect densities, we fabricated hole-only devices with the structure of ITO/PEDOT:PSS/perovskite/spiro-OMeTAD/Au. As a result, the perovskite with OAN<sub>3</sub> showed  $V_{TFL}$  of 0.26 V and  $N_t$  of  $3.68 \times 10^{15} \text{ cm}^{-3}$ . In contrast, the perovskite without OAN<sub>3</sub> showed a larger  $V_{TFL}$  value of 0.36 V and  $N_t$  of  $5.09 \times 10^{15} \text{ cm}^{-3}$ , indicating that OAN<sub>3</sub> could passivate the perovskite surface effectively. From the aforementioned results, we could confirm that the OAN<sub>3</sub> could impart positive effects on perovskite crystals.<sup>51,52</sup>

We fabricated PSCs with OAN<sub>3</sub> using the following configuration: ITO/SnO<sub>2</sub>/(FAPbI<sub>3</sub>)<sub>0.95</sub>(MAPbBr<sub>3</sub>)<sub>0.05</sub>/OAN<sub>3</sub>/P3HT/Au(Ag) (Fig. 1 and S9<sup>†</sup>). We first optimized the concentration of P3HT and OAN<sub>3</sub> to find out the optimal composition (Fig. S10 and S11<sup>†</sup>). Finally, we have fabricated PSCs with the optimal composition (Fig. 4a and Table 1). The OAN<sub>3</sub> device exhibited a PCE of 20.0% with short-circuit current ( $J_{SC}$ ) of  $23.2 \text{ mA cm}^{-2}$ ,

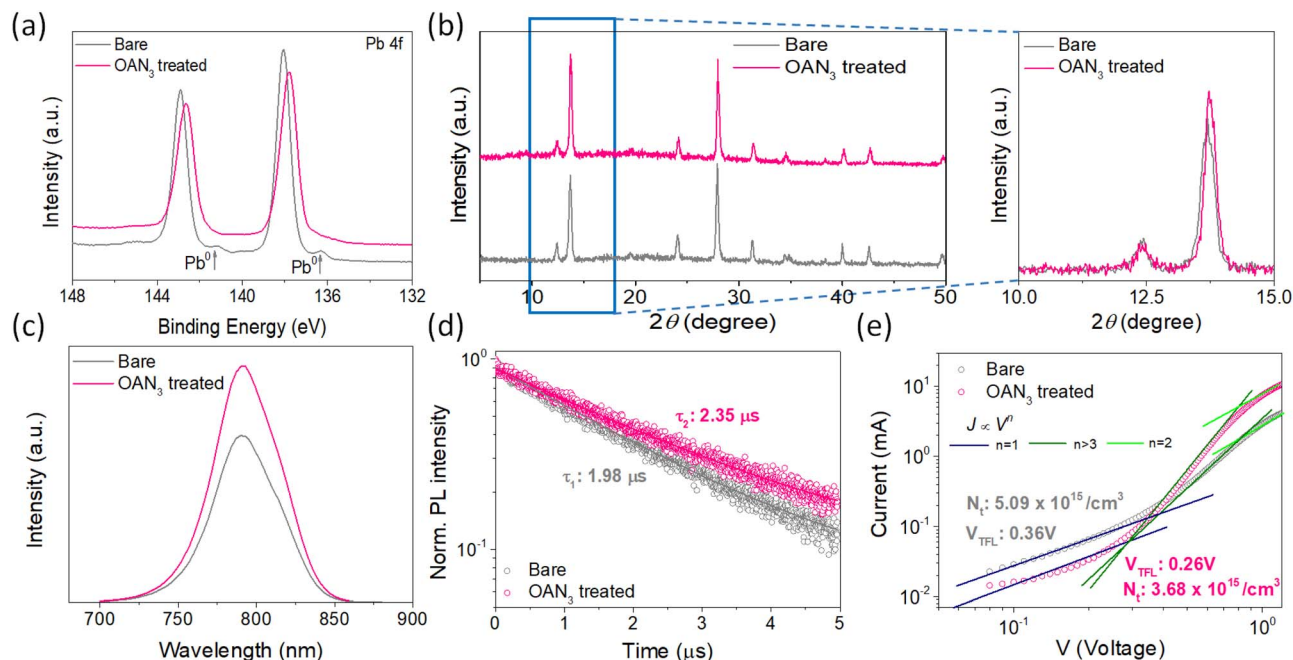


Fig. 3 (a) XPS spectrum of Pb 4f before and after OAN<sub>3</sub> introduction. (b) XRD spectrum of perovskite film under various conditions. (c) Steady-state and (d) time-resolved photoluminescence schematic illustration of perovskite solar cells with and without OAN<sub>3</sub>. (e) Space charge limited current measurement for hole-only devices with and without OAN<sub>3</sub>.

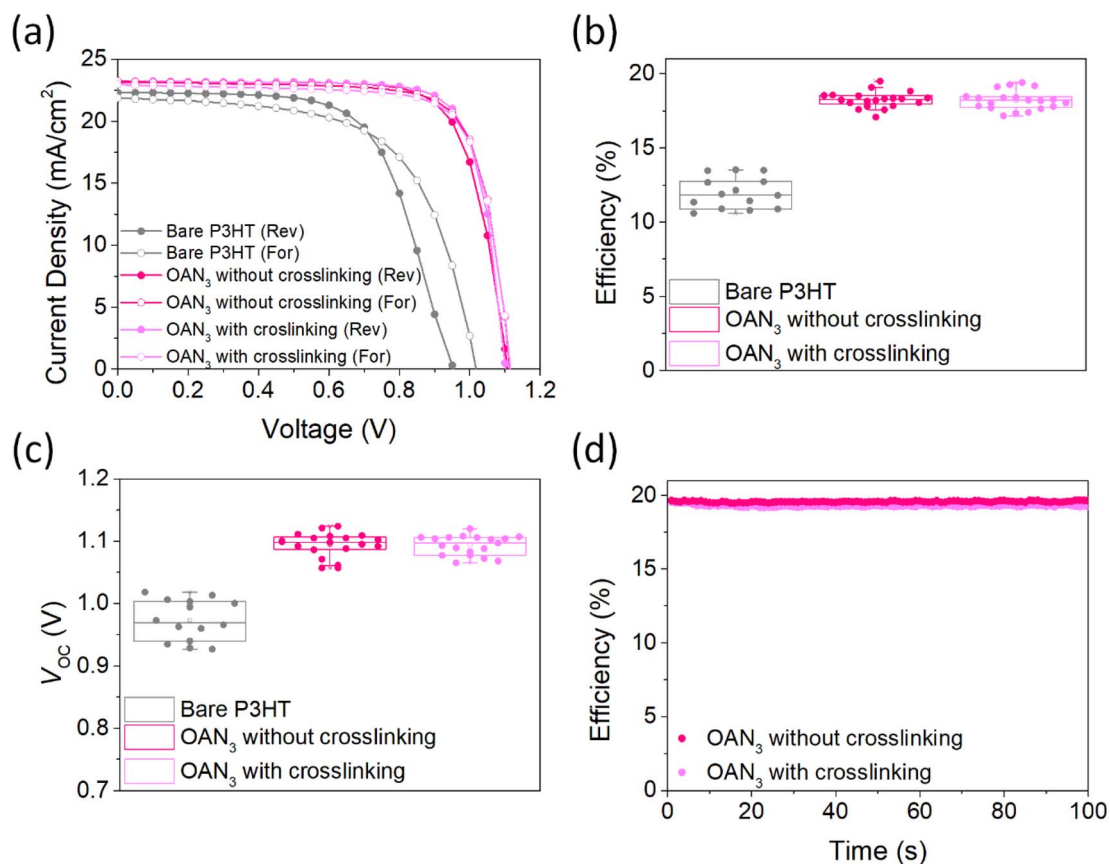


Fig. 4 (a)  $J$ - $V$  curve of champion PSCs before and after OAN<sub>3</sub> introduction. Histogram of (b) power conversion efficiency and (c)  $V_{OC}$  before and after OAN<sub>3</sub> introduction. (d) Stabilized power output before and after OAN<sub>3</sub> introduction.

Table 1 Photovoltaic parameters of the champion PSCs with and without OAN<sub>3</sub>, and before and after crosslinking

Perovskite	Scan direction	$J_{SC}$ [mA cm <sup>-2</sup> ]	$V_{OC}$ [V]	FF [%]	PCE [%]
Bare	Reverse	22.3	0.96	64.2	13.6
	Forward	22.0	1.02	62.0	13.8
OAN <sub>3</sub> without crosslinking	Reverse	23.2	1.12	76.9	20.0
	Forward	23.2	1.11	76.1	19.7
OAN <sub>3</sub> with crosslinking	Reverse	23.1	1.11	77.1	19.8
	Forward	23.0	1.12	76.5	19.7

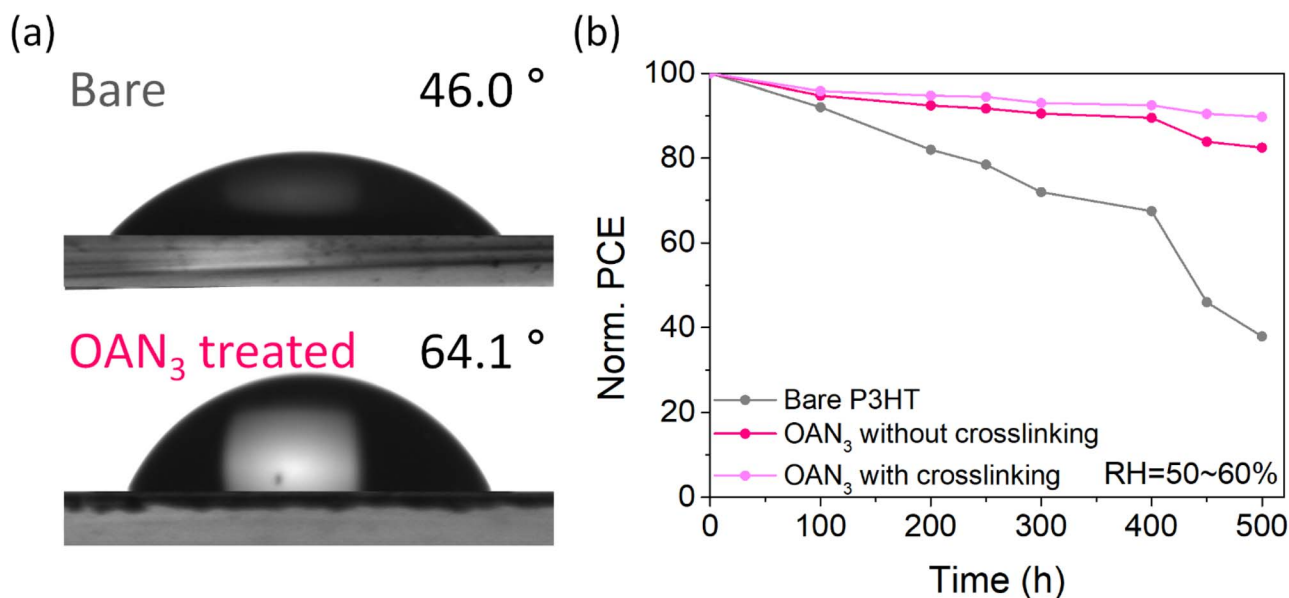


Fig. 5 (a) Contact angles of perovskite film before and after OAN<sub>3</sub> treatment. (b) Moisture-stability under RH: 50–60% storage for PSCs with bare, OAN<sub>3</sub> treated non-crosslinking, and after crosslinking.

open-circuit voltage ( $V_{OC}$ ) of 1.12 V, and fill factor (FF) of 76.9%. The pristine device obtained a PCE of 13.8%,  $J_{SC}$  of 22.0 mA cm<sup>-2</sup>,  $V_{OC}$  of 1.02 V, and FF of 62%. Furthermore, the PSCs with OAN<sub>3</sub> after crosslinking achieved 19.8 ( $J_{SC}$  of 23.1 mA cm<sup>-2</sup>,  $V_{OC}$  of 1.11 V, and FF of 77.1%), which indicates that crosslinking does not deteriorate the efficiency of PSCs. In the photovoltaic histograms of PSCs with OAN<sub>3</sub>, we have confirmed that the  $V_{OC}$  and FF are the major factors in achieving higher efficiency compared to bare PSCs (Fig. 4b, c and S12<sup>†</sup>). This improvement resulted from a synergistic effect between suppressed trap density, reduced non-radiative recombination, and improved crystallinity of perovskite crystal. In addition, we have measured the external quantum efficiency (EQE) spectra, and the integrated  $J_{SC}$  for the OAN<sub>3</sub> device (22.8 mA cm<sup>-2</sup>) well-matched with the value obtained from the  $J-V$  curves (Fig. S13<sup>†</sup>). We further examined the stabilized power output test for the PSCs with OAN<sub>3</sub> (Fig. 4d). PSCs with OAN<sub>3</sub> achieved a PCE of 19.8% and 19.5% before and after crosslinking, respectively.

Finally, the long-term stability of the PSCs was measured by keeping the devices under humid conditions. To confirm the moisture-resistivity of perovskites before and after P3HT, we measured the contact angles for the perovskite with and without OAN<sub>3</sub> (Fig. 5a). The contact angle for the perovskite film

with OAN<sub>3</sub> showed a higher angle of 64.1°, compared to that of the bare perovskite film (46.0°). After that, the unencapsulated devices were stored in RH 50–60% under ambient conditions. The OAN<sub>3</sub>-based devices (with and without crosslinking, respectively) retained 90% and 82% of their initial PCE after 500 h. In contrast, the pristine device only maintained 38% of the initial PCE during the same period (Fig. 5b, S14 and S15<sup>†</sup>). We consider that crosslinking of P3HT and OAN<sub>3</sub> can improve long-term stability by preventing interfacial delamination, which is one of the major factors for PSC degradation.<sup>53,54</sup> These results demonstrate that our strategy of using a crosslinkable molecule (OAN<sub>3</sub>) could achieve highly stable and efficient P3HT-based PSCs.

## Conclusions

In this study, we newly designed and synthesized a small molecule, octylammonium azide (OAN<sub>3</sub>). The ammonium ion is able to passivate the defects in perovskite, and the azide group could provide a crosslinking site with P3HT, strengthening the interfacial contact between perovskite and HTM. As a result, the P3HT with OAN<sub>3</sub> device showed a PCE of 20.0%, which is mainly owing to an improved  $V_{OC}$  and FF compared to the control

device (13.8%). Moreover, the OAN<sub>3</sub>-P3HT PSCs maintained 90% and 82% of initial efficiency after 500 h under 50–60% relative humidity without encapsulation. In contrast, the bare PSCs retained only 38% of initial efficiency after the same period of time. We believe that OAN<sub>3</sub> treatment and cross-linking strategy could endow a high robustness of the PSCs against moisture due to the increased hydrophobicity and compact interfacial contact between perovskite and P3HT. Our dual-functional molecule strategy could provide a guideline to develop novel species of surface modifiers, which could improve the efficiency and stability simultaneously.

## Author contributions

S. Song designed and organized the project. The experiments were carried out by H. Choi, H. Lim, H. Kim, J. Lim, M. Park, and C. S. Pathak with the guidance of S. Song. The OAN<sub>3</sub> molecule was synthesized and characterized by H. Lim. The perovskite solar cells were fabricated by H. Choi, H. Kim, and J. Lim and analysed by H. Choi, M. Park, and C. S. Pathak under comments of S. Song. Lastly, the manuscript was written by H. Choi and H. Lim and advised by S. Song.

## Conflicts of interest

There are no conflicts to declare.

## Acknowledgements

This work was supported by the Technology Development Program (S3324563) funded by the Ministry of SMEs and Startups (MSS, Korea), by the National Research Foundation of Korea (NRF) grant by the Ministry of Education (NRF-2022R1F1A1074465), and Korea government (MSIT) (2022M3J1A1064317).

## References

- L. Chouhan, S. Ghimire, C. Subrahmanyam, T. Miyasaka and V. Biju, *Chem. Soc. Rev.*, 2020, **49**, 2869–2885.
- J. Y. Kim, J.-W. Lee, H. S. Jung, H. Shin and N.-G. Park, *Chem. Rev.*, 2020, **120**, 7867–7918.
- P. V. Shinde, A. Patra and C. S. Rout, *J. Mater. Chem. C*, 2022, **10**, 10196–10223.
- NREL, *Best Research-Cell Efficiency Chart*, <https://www.nrel.gov/pv/assets/pdfs/best-research-cell-efficiencies.pdf>, accessed March, 2023.
- L. Meng, J. You and Y. Yang, *Nat. Commun.*, 2018, **9**, 5265.
- Y. Cheng and L. Ding, *Energy Environ. Sci.*, 2021, **14**, 3233–3255.
- N. Li, X. Niu, Q. Chen and H. Zhou, *Chem. Soc. Rev.*, 2020, **49**, 8235–8286.
- J. Yang, B. D. Siempelkamp, D. Liu and T. L. Kelly, *ACS Nano*, 2015, **9**, 1955–1963.
- K. Choi, J. Lee, H. Choi, G.-W. Kim, H. I. Kim and T. Park, *Energy Environ. Sci.*, 2020, **13**, 5059–5067.
- H. Min, D. Y. Lee, J. Kim, G. Kim, K. S. Lee, J. Kim, M. J. Paik, Y. K. Kim, K. S. Kim, M. G. Kim, T. J. Shin and S. I. Seok, *Nature*, 2021, **598**, 444–450.
- T. Zhang, F. Wang, H.-B. Kim, I.-W. Choi, C. Wang, E. Cho, R. Konefal, Y. Puttison, K. Terado, L. Kobera, M. Chen, M. Yang, S. Bai, B. Yang, J. Suo, S.-C. Yang, X. Liu, F. Fu, H. Yoshida, W. M. Chen, J. Brus, V. Coropceanu, A. Hagfeldt, J.-L. Brédas, M. Fahlman, D. S. Kim, Z. Hu and F. Gao, *Science*, 2022, **377**, 495–501.
- J. J. Yoo, G. Seo, M. R. Chua, T. G. Park, Y. Lu, F. Rotermund, Y.-K. Kim, C. S. Moon, N. J. Jeon, J.-P. Correa-Baena, V. Bulović, S. S. Shin, M. G. Bawendi and J. Seo, *Nature*, 2021, **590**, 587–593.
- R. Sun, Q. Tian, M. Li, H. Wang, J. Chang, W. Xu, Z. Li, Y. Pan, F. Wang and T. Qin, *Adv. Funct. Mater.*, 2023, **33**, 2210071.
- W. H. Nguyen, C. D. Bailie, E. L. Unger and M. D. McGehee, *J. Am. Chem. Soc.*, 2014, **136**, 10996–11001.
- J. Lee, M. M. Byranvand, G. Kang, S. Y. Son, S. Song, G.-W. Kim and T. Park, *J. Am. Chem. Soc.*, 2017, **139**, 12175–12181.
- G.-W. Kim, G. Kang, J. Kim, G.-Y. Lee, H. I. Kim, L. Pyeon, J. Lee and T. Park, *Energy Environ. Sci.*, 2016, **9**, 2326–2333.
- S. Wang, Z. Huang, X. Wang, Y. Li, M. Günther, S. Valenzuela, P. Parikh, A. Cabrerros, W. Xiong and Y. S. Meng, *J. Am. Chem. Soc.*, 2018, **140**, 16720–16730.
- A. K. Jena, M. Ikegami and T. Miyasaka, *ACS Energy Lett.*, 2017, **2**, 1760–1761.
- N. J. Jeon, H. Na, E. H. Jung, T.-Y. Yang, Y. G. Lee, G. Kim, H.-W. Shin, S. I. Seok, J. Lee and J. Seo, *Nat. Energy*, 2018, **3**, 682–689.
- S.-Y. Jeong, H.-S. Kim and N.-G. Park, *ACS Appl. Mater. Interfaces*, 2022, **14**, 34220–34227.
- T. K. Zhang, F. Wang, H. B. Kim, I. W. Choi, C. F. Wang, E. Cho, R. Konefal, Y. Puttison, K. Terado, L. Kobera, M. Y. Chen, M. Yang, S. Bai, B. W. Yang, J. J. Suo, S. C. Yang, X. J. Liu, F. Fu, H. Yoshida, W. M. M. Chen, J. Brus, V. Coropceanu, A. Hagfeldt, J. L. Bredas, M. Fahlman, D. S. Kim, Z. J. Hu and F. Gao, *Science*, 2022, **377**, 495.
- W. H. Nguyen, C. D. Bailie, E. L. Unger and M. D. McGehee, *J. Am. Chem. Soc.*, 2014, **136**, 10996.
- J. Kong, Y. Shin, J. A. Röhr, H. Wang, J. Meng, Y. Wu, A. Katzenberg, G. Kim, D. Y. Kim, T. D. Li, E. Chau, F. Antonio, T. Siboonruang, S. Kwon, K. Lee, J. R. Kim, M. A. Modestino, H. Wang and A. D. Taylor, *Nature*, 2021, **594**, 51.
- F. M. Rombach, S. A. Haque and T. J. Macdonald, *Energy Environ. Sci.*, 2021, **14**, 5161–5190.
- L. Caliò, M. Salado, S. Kazim and S. Ahmad, *Joule*, 2018, **2**, 1800–1815.
- T. Zhang, F. Wang, H.-B. Kim, I.-W. Choi, C. Wang, E. Cho, R. Konefal, Y. Puttison, K. Terado, L. Kobera, M. Chen, M. Yang, S. Bai, B. Yang, J. Suo, S.-C. Yang, X. Liu, F. Fu, H. Yoshida, W. M. Chen, J. Brus, V. Coropceanu, A. Hagfeldt, J.-L. Brédas, M. Fahlman, D. S. Kim, Z. Hu and F. Gao, *Science*, 2022, **377**, 495–501.

- 27 X. Ji, T. Zhou, X. Ke, W. Wang, S. Wu, M. Zhang, D. Lu, X. Zhang and Y. Liu, *J. Mater. Chem. A*, 2020, **8**, 5163–5170.
- 28 G.-W. Kim, G. Kang, K. Choi, H. Choi and T. Park, *Adv. Energy Mater.*, 2018, **8**, 1801386.
- 29 G.-W. Kim, J. Lee, G. Kang, T. Kim and T. Park, *Adv. Energy Mater.*, 2018, **8**, 1701935.
- 30 W. Wang, J. Zhou and W. Tang, *J. Mater. Chem. A*, 2022, **10**, 1150–1178.
- 31 G. Qu, L. Dong, Y. Qiao, D. Khan, Q. Chen, P. Xie, X. Yu, X. Liu, Y. Wang, J. Chen, X. Chen and Z.-X. Xu, *Adv. Funct. Mater.*, 2022, **32**, 2206585.
- 32 J. Lee, G.-W. Kim, M. Kim, S. A. Park and T. Park, *Adv. Energy Mater.*, 2020, **10**, 1902662.
- 33 Q. Fu, X. Tang, H. Liu, R. Wang, T. Liu, Z. Wu, H. Y. Woo, T. Zhou, X. Wan, Y. Chen and Y. Liu, *J. Am. Chem. Soc.*, 2022, **144**, 9500–9509.
- 34 E. H. Jung, N. J. Jeon, E. Y. Park, C. S. Moon, T. J. Shin, T.-Y. Yang, J. H. Noh and J. Seo, *Nature*, 2019, **567**, 511–515.
- 35 D. Xu, Z. Gong, Y. Jiang, Y. Feng, Z. Wang, X. Gao, X. Lu, G. Zhou, J.-M. Liu and J. Gao, *Nat. Commun.*, 2022, **13**, 7020.
- 36 S. S. Mali, J. V. Patil, J. A. Steele, S. R. Rondiya, N. Y. Dzade and C. K. Hong, *ACS Energy Lett.*, 2021, **6**, 778–788.
- 37 J. Song, H. Xie, E. L. Lim, Y. Li, T. Kong, Y. Zhang, X. Zhou, C. Duan and D. Bi, *Sol. RRL*, 2022, **6**, 2100880.
- 38 Q. K. Hu, E. Rezaee, Q. S. Dong, H. Q. Shan, Q. Chen, L. D. Wang, B. C. Liu, J. H. Pan and Z. X. Xu, *Sol. RRL*, 2019, **3**, 1800264.
- 39 C. M. Pelicano and H. Yanagi, *J. Energy Chem.*, 2018, **27**, 455–462.
- 40 Y. Zhang, M. Elawad, Z. Yu, X. Jiang, J. Lai and L. Sun, *RSC Adv.*, 2016, **6**, 108888–108895.
- 41 M. J. Jeong, K. M. Yeom, S. J. Kim, E. H. Jung and J. H. Noh, *Energy Environ. Sci.*, 2021, **14**, 2419–2428.
- 42 M.-H. Li, J.-Y. Shao, Y. Jiang, F.-Z. Qiu, S. Wang, J. Zhang, G. Han, J. Tang, F. Wang, Z. Wei, Y. Yi, Y.-W. Zhong and J.-S. Hu, *Angew. Chem., Int. Ed.*, 2021, **60**, 16388–16393.
- 43 J. J. Yoo, S. Wiegold, M. C. Sponseller, M. R. Chua, S. N. Bertram, N. T. P. Hartono, J. S. Tresback, E. C. Hansen, J.-P. Correa-Baena, V. Bulović, T. Buonassisi, S. S. Shin and M. G. Bawendi, *Energy Environ. Sci.*, 2019, **12**, 2192–2199.
- 44 Q. Jiang, Y. Zhao, X. Zhang, X. Yang, Y. Chen, Z. Chu, Q. Ye, X. Li, Z. Yin and J. You, *Nat. Photonics*, 2019, **13**, 460–466.
- 45 M. J. Kim, M. Lee, H. Min, S. Kim, J. Yang, H. Kweon, W. Lee, D. H. Kim, J.-H. Choi, D. Y. Ryu, M. S. Kang, B. Kim and J. H. Cho, *Nat. Commun.*, 2020, **11**, 1520.
- 46 B. Liu, R.-Q. Png, L.-H. Zhao, L.-L. Chua, R. H. Friend and P. K. H. Ho, *Nat. Commun.*, 2012, **3**, 1321.
- 47 S. Song, E. Y. Park, B. S. Ma, D. J. Kim, H. H. Park, Y. Y. Kim, S. S. Shin, N. J. Jeon, T. S. Kim and J. Seo, *Adv. Energy Mater.*, 2021, **11**, 2003382.
- 48 W. Zhao, J. Xu, K. He, Y. Cai, Y. Han, S. Yang, S. Zhan, D. Wang, Z. Liu and S. Liu, *Nano-Micro Lett.*, 2021, **13**, 169.
- 49 Y. Zhou, Z. Wang, J. Jin, X. Zhang, J. Zou, F. Yao, Z. Zhu, X. Cui, D. Zhang, Y. Yu, C. Chen, D. Zhao and Q. Cao, *Angew. Chem.*, 2023, **135**, e202300759.
- 50 W.-M. Gu, K.-J. Jiang, F. Li, G.-H. Yu, Y. Xu, X.-H. Fan, C.-Y. Gao, L.-M. Yang and Y. Song, *Chem. Eng. J.*, 2022, **444**, 136644.
- 51 X. Ding, H. Wang, C. Chen, H. Li, Y. Tian, Q. Li, C. Wu, L. Ding, X. Yang and M. Cheng, *Chem. Eng. J.*, 2021, **410**, 128328.
- 52 H. Wang, W. Zhang, B. Wang, Z. Yan, C. Chen, Y. Hua, T. Wu, L. Wang, H. Xu and M. Cheng, *Nano Energy*, 2023, **111**, 108363.
- 53 J. H. Yun, I. Lee, T.-S. Kim, M. J. Ko, J. Y. Kim and H. J. Son, *J. Mater. Chem. A*, 2015, **3**, 22176–22182.
- 54 R. Ichwani, V. Uzonwanne, A. Huda, R. Koech, O. K. Oyewole and W. O. Soboyejo, *ACS Appl. Energy Mater.*, 2022, **5**, 6011–6018.